

# Production of yttrium aluminum silicate microspheres by gelation of an aqueous solution containing yttrium and aluminum ions in silicone oil

M.R. Ghahramani\*, A.A. Garibov, T.N. Agayev

Institute of Radiation Problems, Azerbaijan National Academy of Sciences, Baku, Azerbaijan

## ABSTRACT

**Background:** Radioactive yttrium glass microspheres are used for liver cancer treatment. These yttrium aluminum silicate microspheres are synthesized from yttrium, aluminum and silicone oxides by melting. There are two known processes used to transform irregular shaped glass particles into microspheres, these 'spheroidization by flame' and 'spheroidization by gravitational fall in a tubular furnace'. **Materials and Methods:** Yttrium aluminum silicate microspheres with the approximate size of 20-50  $\mu\text{m}$  were obtained when an aqueous solution of  $\text{YCl}_3$  and  $\text{AlCl}_3$  was added to tetraethyl orthosilicate (TEOS) and pumped in to silicone oil and stirred constantly the temperature of 80°C. The resulting spherical shapes were then investigated for crystallization, chemical bonds, composition and distribution of elements by scanning electron microscopy (SEM), X-ray diffraction (XRD), Fourier transform infrared spectroscopy (FTIR), carbon/sulfur analysis, X-ray photoelectron spectroscopy (XPS) and SEM/EDS analysis. **Results:** The particles produced by the above-mentioned method were regular and nearly spherical in shape. The results of topographical analysis of a cross-section showed that form of the microspheres had formed a 'boiled egg' structure. This method has an advantage over other methods in that the process does not require high temperatures. **Conclusion:** This paper reports on a novel method to produce yttrium glass microspheres. The resulting microspheres were formed with a silicon crust so the proposed method is expected to be suitable for application in the production of radioactive seed sources for implantation in tumors and cancer tissue.

**Keywords:** Yttrium microspheres, brachytherapy microspheres, seed source, sol gel technique.

## ► Original article

### \* Corresponding author:

Dr. M.R. Ghahramani,

Fax: +99 41 25398318

E-mail:

[ghahramani.mr@gmail.com](mailto:ghahramani.mr@gmail.com)

Received: July 2013

Accepted: Oct. 2013

*Int. J. Radiat. Res.*, April 2014;  
12(2): 179-187

## INTRODUCTION

Cancer is commonly treated by complete removal of the diseased tissue but unfortunately this seldom leads to recovery or return of full tissue function. Noninvasive techniques for cancer treatment were introduced in the mid 1980s, in which only the cancer cells are destroyed. In 1987, radioactive glass microspheres of  $^{177}\text{Lu}_2\text{O}_3\text{-}^{19}\text{Al}_2\text{O}_3\text{-}^{64}\text{SiO}_2$  (mol %), 20-30  $\mu\text{m}$  in diameter, were shown to be

effective for in situ radiotherapy treatment of liver cancer (1-12). Yttrium-89 in glass can be transformed into the  $\beta$ -emitter  $^{90}\text{Y}$  using neutron bombardment. Specifically,  $^{90}\text{Y}$  has a half-life of 64.1 h, and other elements in the glass are not activated from neutron bombardment. When these 20-30  $\mu\text{m}$  diameter radioactive glass microspheres are injected into a target organ or tissue (e.g., a liver tumor), they become trapped inside the small blood vessels of the tumor and tend to block supplies of nutrition to the tumor in addition to providing a large, localized dose of

short-range, highly ionizing  $\beta$ -rays to the tumor. The  $\beta$ -rays do not affect any other chemical elements and have a short penetration range of only approximately 2.55 mm in living tissue, so there is little danger of radiation to neighboring healthy tissue <sup>(13)</sup>. Glass is insoluble in body fluids and non-toxic <sup>(15)</sup>. Glass microspheres have been investigated in clinical trials for irradiation of diseased kidneys and malignant tumors in the liver and for radiation synovectomy of arthritic joints <sup>(4)</sup>.

These microspheres can be produced in various forms; biodegradable polymer, ion exchange resins or ceramic (glass) materials <sup>(8)</sup>. There are two types of microsphere devices containing <sup>90</sup>Y that are currently commercially available; one glass microspheres (Thera-Sphere; MDS Nordion, Ottawa, Ontario, Canada) and the other of resin microspheres (SIR-Spheres; Sirtex Medical, Sydney, Australia). The effective use of resin microspheres may be compromised as there can be trace amounts of free <sup>90</sup>Y on the surface due to leaching, and perhaps as much as 0.4% of <sup>90</sup>Y activity is excreted in urine during the first 24 h after administration of a treatment. Research has shown that urinary excretion of trace amounts (25–50 kBq/L/GBq) of radionuclides is a possibility during the first 24 hrs after implantation <sup>(34)</sup>. The problem with the melting method for synthesizing yttrium aluminum silicate microspheres from yttrium, aluminum and silicon oxides is that it requires high temperatures (>1600°C) <sup>(1, 12-14)</sup>. It is therefore difficult to control purity and homogeneity of the yttrium synthesized under these conditions, whereas the sol-gel method avoids such problems.

Spherical particles reduce or prevent the formation of particle clusters within peripheral vessels and facilitate deeper penetration in the neoplasm vasculature, providing permanent and effective staining <sup>(21)</sup>. Irregular shaped glass particles have been transformed into microspheres using two different processes <sup>(1, 12-14)</sup>. In the first process, glass microspheres with particle size distribution of 20–150  $\mu$ m were obtained by re-melting irregular particles in a hot flame. This process was done using a

torch to burn a mixture of oxygen and liquefied petrol gas. The microspheres were collected in a metal cylinder. Although this process, known as spheroidization by flame, has been previously reported, optimal results can only be achieved by adjusting the experimental parameters for each type of glass used in the process. The second process consists of introducing irregular shaped glass particles into the top of a vertical tubular furnace and allowing the particles to fall inside the furnace. This process is commonly referred to as spheroidization by gravitational fall in a tubular furnace.

## MATERIALS AND METHODS

### *Microspheres production*

Yttrium chloride ( $YCl_3$ ) was produced by the reaction of yttrium oxide (99.99%, Aldrich, Cat. No. 205168) with hydrochloric acid (37%, Merck, Cat. No. 109973).  $SiO_2$  colloids were produced by adding TEOS (99%, Aldrich, Cat. No. 86578) to water at room temperature and stirred constantly. The molar composition of TEOS:  $CH_3COOH$ : $H_2O$  was 1: 0.5: 1, which was determined as the optimum composition to obtain an yttrium aluminum silicate sol. Y and Al ions were incorporated into the  $SiO_2$  by substituting water for aqueous solutions of  $YCl_3$  and  $AlCl_3$ , respectively.

The sol preparations were loaded into a syringe and pumped through a 0.4 mm diameter nozzle into silicone oil (Shenzhen Hong Ye Jie Technology Co., Ltd.) then heated to the temperature of 80 °C under constant magnetic stirring (500 rpm). The sol droplets were converted into spheres in silicone oil by the forces of surface tension. These microsols converted to a solid state after 30 min in the silicon.

Microspheres were separated from the silicone oil by precipitation and washed with 30 ml of petroleum ether. This process was repeated at least three times. They were then washed with 10 ml of diethyl ether to remove any trace of silicone oil from surfaces. The microspheres were finally washed with 100 ml of water.

Remaining acids and other additives were removed from the microspheres by heating in a furnace up to the temperature of 800 °C for 3 hrs. The temperature was increased by 5°C/min until it reached 800 °C; after 3 hrs, the temperature was decreased by 10°C/min.

This study presents a method for producing spherical glass micro particles using a method employing silicone oil. The yttrium microspheres obtained by this proposed method are termed azar spheres. These obtained yttrium silicate microspheres and yttrium aluminum silicate microspheres have been named Azar sphere 1 and Azar sphere 2, respectively. This work was done to develop a method spheroidization to produce yttrium aluminum silicate micro particles without the use of high temperatures.

Stability of the crystalline phase after heat treatment was investigated with XRD. Absorption bands of the mineral phase were studied using Fourier transform infrared spectroscopy (FTIR). XRF analysis was done to determine elemental composition on the products. A carbon/sulfur determinator was used to determine amounts of carbon present. SEM/EDS mapping and line scan analysis were used to determine distributions of elements in cross sections of the microspheres.

#### X-ray diffraction analysis

Crystallization of samples was determined from analysis by, X-ray diffraction (XRD) (Siemens D1666, Cu-K $\alpha$  radiation) after heat-treatments at 800 °C and 1000 °C. Figure 1 shows the XRD patterns after heat treatment at 800°C. Figure 2 shows the XRD patterns after heat treatment at 1000 °C.

#### Fourier transform infrared spectroscopy

Chemical bonds were determined from analysis by Fourier transform infrared spectroscopy (FTIR) (TENSOR27, Bruker). For the FTIR spectra, a 2 mg of each sample was added to 300 mg of spectral grade potassium bromide (KBr). These mixtures were then ground and pressed to form transparent disks. The technique of transmittance was used to scan the samples. Figure 3 shows FTIR spectra

in the range of 350-4000 cm<sup>-1</sup> after heat treatment at 800 °C for 3 h.

#### X-ray photoelectron spectroscopy

Microsphere stoichiometry was determined according to the XPS spectrum using Si 2p, Y 3d and O 1s bond energies. Figures 4-5 show the survey spectra for the Azar samples. The

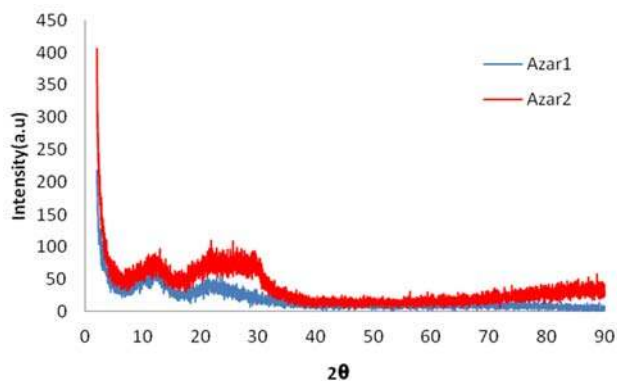


Figure 1. XRD patterns of the Azar 1 and Azar 2 samples after heat treatment at 800 °C for 3 h.

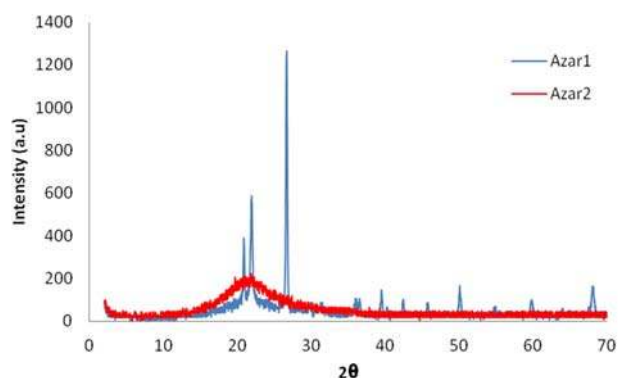


Figure 2. XRD spectra of the Azar 1 and Azar 2 samples after heat treatment at 1000 °C for 3 h.

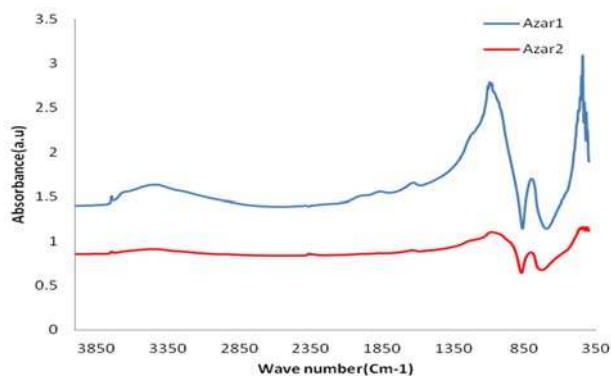


Figure 3. The FTIR spectra of the microspheres after heat treatment at 800 °C for 3 h.

absolute bond energies of the O 1s, Y 3d and Si 2s photoelectron peaks were determined with respect to the C 1s transition at 284.2 eV.

Figure 4a-e shows the chemical bonding states for silicon, yttrium and oxygen. Evaluations of absorbed peaks in these states were 102.93, 153.44 and 532.55 eV, respectively.

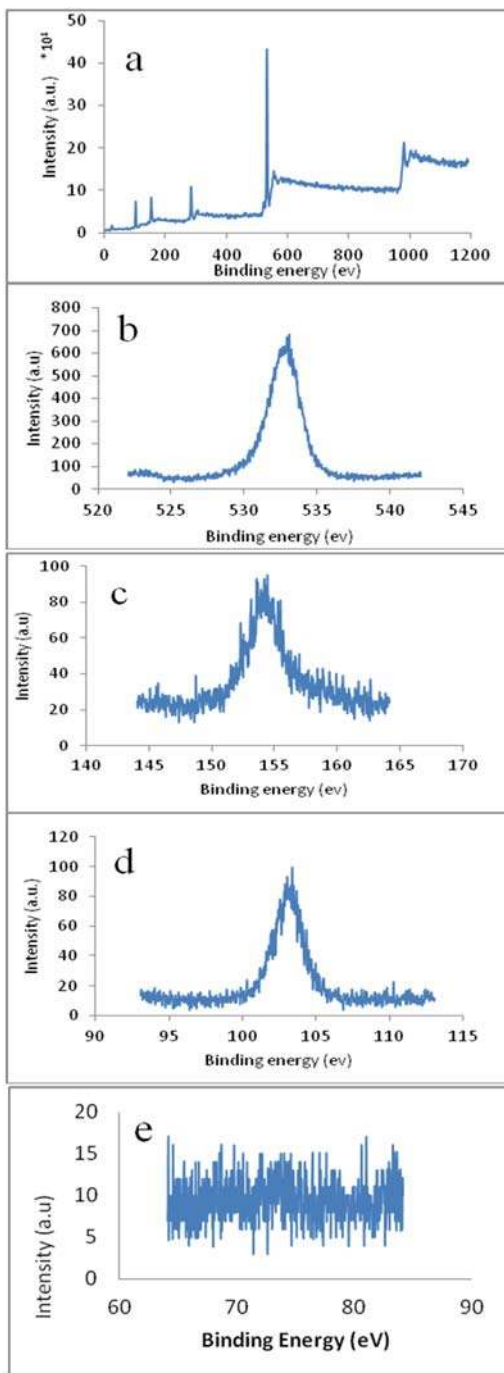


Figure 4. The XPS analysis of the Azar 1 samples.

Figure 5a-d shows chemical bonds of 103.4, 154.4 and 533.1 eV in the silicon, yttrium and oxygen states, respectively. Figure 4e determines no evidence of peaks in the aluminum state.

### Scanning electron microscopy

Approximately 1 mg of dry powder was placed on a 1-cm<sup>2</sup> glass slide, and two droplets of petroleum ether were added to distribute the powder evenly on to the surface of a glass slide. After drying, samples were sputter-coated with Au-Pd for SEM analysis to reduce electrostatic interaction. SEM analysis was performed by scanning electron microscopy (VEGA\TESCAN-XMU).

SEM images of samples were produced both with and without application of the proposed silicone oil method; these are shown in figures 6 and 7, respectively. Figure 6 shows a micrograph of glass particles prepared without application of the proposed silicone oil method.

In this process, the prepared sol was putted into a vial for 1 day to produce the gel. After

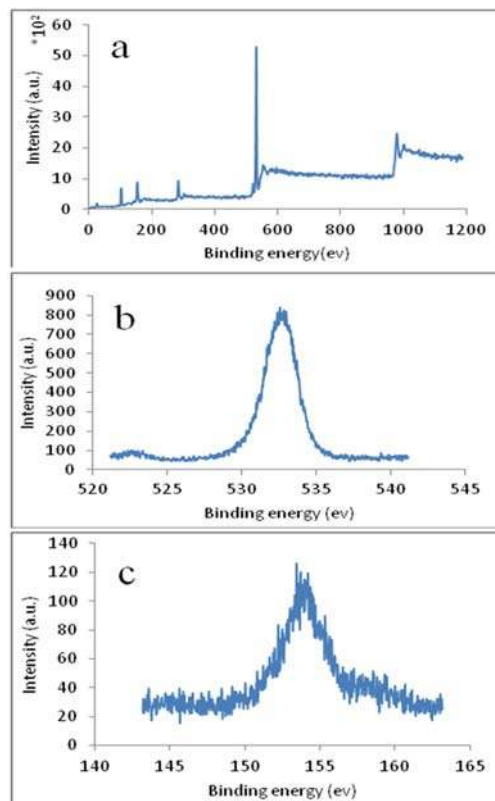


Figure 5. The XPS analysis of the Azar 2 samples.

gelation, it was crushed and annealed at 800 °C for 3 h.

### SEM/EDS mapping analysis

Microsphere samples were mounted to facilitate manipulation during preparation. These powders were mounted in a polycarbonate disc that was 30 mm in diameter and 5 mm long. The technique of compression molding was used to produce hard mounts in a minimum amount of time. Conditions of temperature and pressure were held constant within the mounting press.

The mount was inserted into a polishing tool and held firmly by the operator. The tool was moved 20 times back and forth across abrasive paper in a straight line toward or away from the operator. This process was performed sequentially with water and grit at levels of 1000-, 1500-, 2000-, 2500- and 3000-grit.

SEM/EDS mapping analysis was performed using scanning electron microscopy (VEGA\\TESCAN-LMU). Quantitative analysis of the microstructure of the mounted microspheres was determined by application of SEM mapping, as shown in figures 9-10 that show a topographical analysis of cross-sections of the microspheres. Figures 9-10 also show EDS maps of the Azar microspheres. These EDS maps demonstrate distributions of Y, Si, O for each of the specimens (figure 10) and Al (figure 9) in cross-sections of the microspheres.

### SEM/EDS line scan analysis

SEM/EDS line scan techniques were applied to determine elemental redistributions across cross-sections of the microsphere samples. Figures 11-12 show the SEM/EDX line scan analysis along cross-sections of the Azar samples for various concentrations of Si, Y, O and Al.

### Chemical analysis

Semi-quantitative analysis was performed on the Azar samples in accordance with the ASTM C 982-03 guidelines. X-ray fluorescence spectrometry analysis was performed to identify impurities in chemical elements of the Azar sphere samples. A carbon/sulfur

determinator was used to determine amounts of carbon present in the samples. Tables 1 and 2 show the elements and composition of the Azar microspheres.

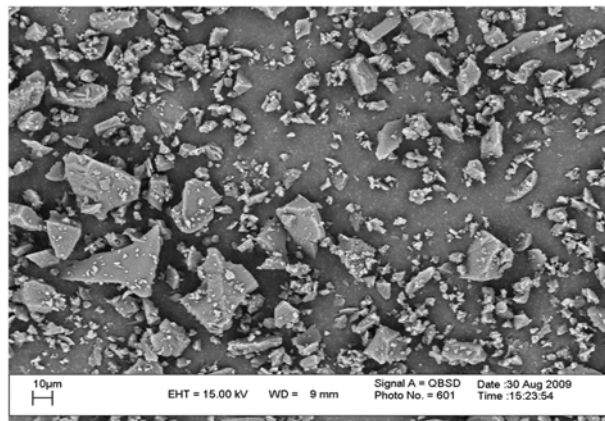


Figure 6. The SEM micrograph of glass particles produced without spheroidization.

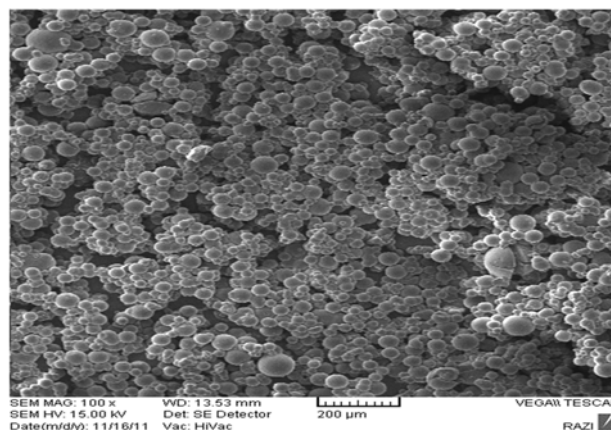


Figure 7. The SEM micrograph of glass particles produced using the silicone oil method of spheroidization.

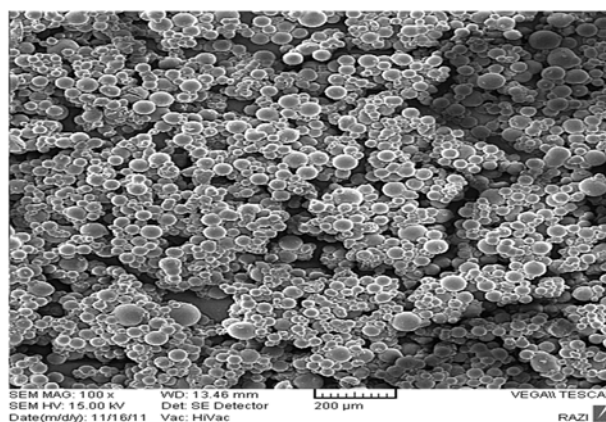


Figure 8. The SEM micrograph of glass particles with a regular shape.

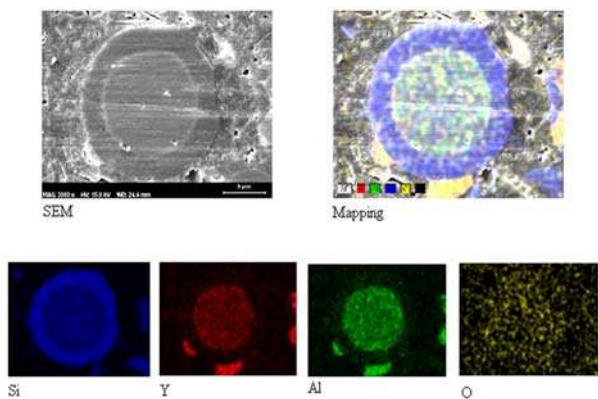


Figure 9. SEM/EDS mapping and topographical analysis of the Azar 1 samples.

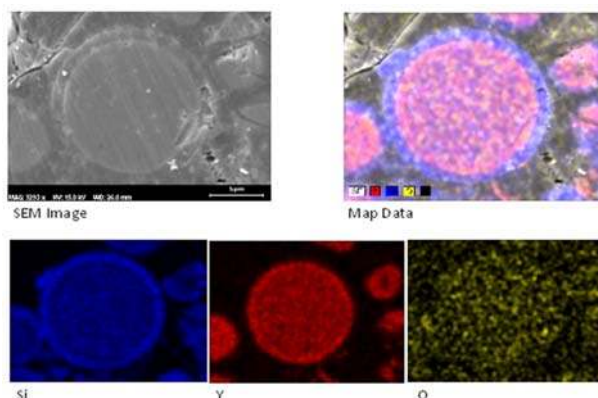


Figure 10. SEM/EDS mapping and topographical analysis of the Azar 2 samples.

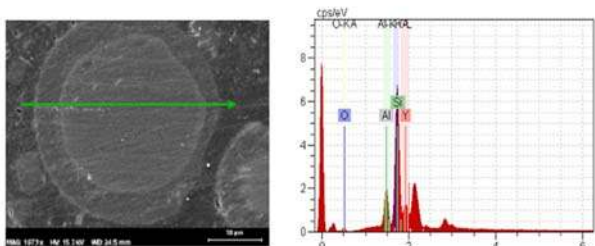
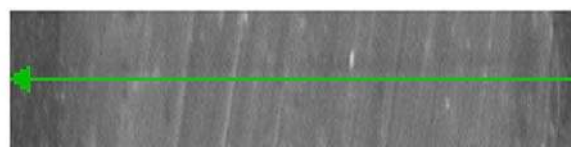
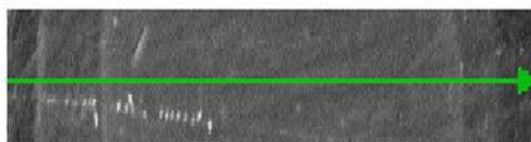
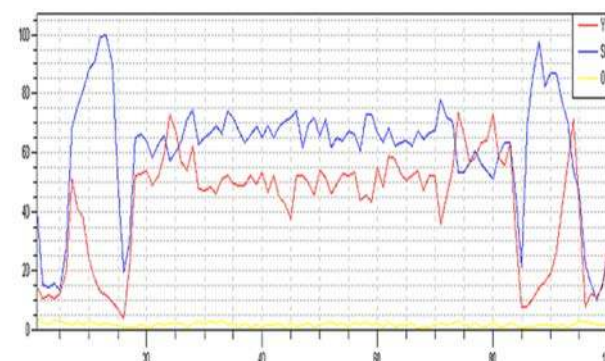
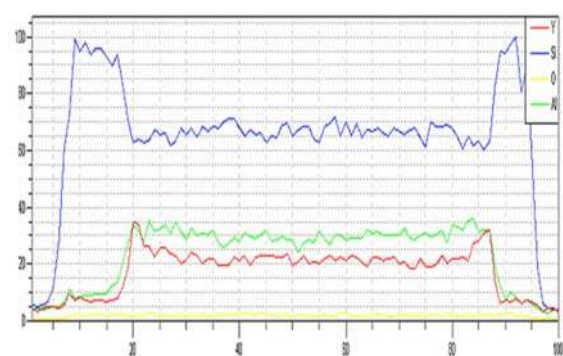


Figure 11. SEM/EDS Line scan analysis of the Azar 1 samples.

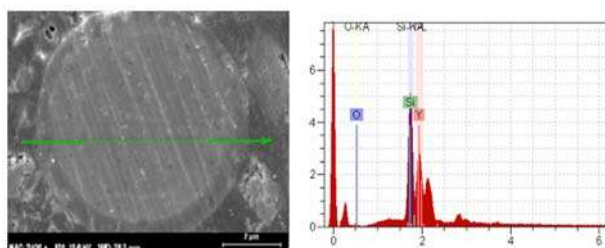


Figure 12. SEM/EDS Line scan analysis of the Azar 2 samples.

Table 1. X-ray fluorescence spectrometry and carbon/Sulfur analysis of samples

Elements	Yttrium (%)	Silicon (%)	Aluminum (%)	La & Lu (%)	Carbon (%)
Azar 1	28.5	23.7	6.9	<1	0.02
Azar 2	52	15.7	-	<1	0.01

Table 2. Azar spheres composition.

Chemical composition	SiO <sub>2</sub> (%)	Y <sub>2</sub> O <sub>3</sub> (%)	Al <sub>2</sub> O <sub>3</sub> (%)
Azar 1	50.7	36.2	13
Azar 2	33.7	66.2	-

## RESULTS

### *X-ray diffraction analysis*

The XRD patterns of samples after heat treatment at 800 °C are shown in figure 1. Patterns shown in figure 1 determine that samples (Azar 1 and Azar 2) were not crystalline. Figure 2 shows the XRD spectra for Azar 1 and Azar 2 samples after heat treatment at 1000 °C for 3 h. Patterns shown in this figure confirm that crystals were formed in the Azar 1 sample at 1000 °C.

From the patterns demonstrated in these figures, it can be concluded that samples were not crystalline and that the glass was stable and showed no evidence of a crystalline phases after heat treatment up to 800°C. This figure also confirms that the yttrium aluminum silicate oxides existed in an amorphous state in the glass microsphere composite up to 800°C. Nucleation of the crystalline phase is undesirable because it can induce stress in the glass structure and interfere with by forming cracks and other defects in the microspheres<sup>(12)</sup>.

### *Fourier transform infrared spectroscopy*

Spectrum for the microspheres (figure 3) clearly shows the absorption bands of the mineral phase, visible in the 700 cm<sup>-1</sup> and 867 cm<sup>-1</sup> regions. Peaks observed at 700 cm<sup>-1</sup> and 867 cm<sup>-1</sup> can be attributed to stretching mode of the bond of Si-O-Y<sup>(16-20)</sup>. Other combinations, such as Y-Si and Al-O, are improbable because they would produce short wavelength peaks or be outside of the measured range.

### *X-ray photoelectron spectroscopy*

XPS analysis of Azar 1 sample presented; Al 2p, Si 2p, Y 3d, and O 1s spectra in figure 4. The peak assigned to the Al 2p level of Al<sub>2</sub>O<sub>3</sub> is 74 eV<sup>(22-24)</sup>. The XPS spectra illustrated in Figure 4e does not indicate the presence of Al-O bonds. The peak (figure 4d) assigned to the Si-O bond (102.93) is close to the Si 2p peak for SiO<sub>2</sub> (103 eV)<sup>(25, 29)</sup>. The O 1s peak (figure 4b) was measured at 532.55 eV and as such is close to the SiO<sub>2</sub> peak (533 eV)<sup>(26-29)</sup>, whereas the peak assigned to the O 1s level for Y<sub>2</sub>O<sub>3</sub> is 529.5 eV<sup>(32,33)</sup>. The Y 3d spectrum exhibited a peak at

153.44 eV (figure 4c), whereas other tests have reported exhibition of a double peak from the spin-orbit splitting of the Y 3d<sub>3/2</sub> and Y 3d<sub>5/2</sub> levels for Y<sub>2</sub>O<sub>3</sub> at 158.8 and 156.8 eV<sup>(5,10,26-29,31)</sup>, respectively. Thus, the peak at 153.44 eV (figure 4c) in the Y 3d spectrum resulted from the Si 2s level<sup>(28-30, 32, 33)</sup>.

Figure 5 presents the Si 2p, Y3d, and O 1s XPS spectra of the Azar 2 sample. The peak (figure 5d) assigned to the Si-O bond (103.4) is close to the Si 2p peak for SiO<sub>2</sub> (103 eV) [25, 29]. The O 1s peak (figure 5b) was measured at 533.1 eV and is close to the SiO<sub>2</sub> peak (533 eV)<sup>(26-29)</sup>, whereas the peak assigned to the O1s level for Y<sub>2</sub>O<sub>3</sub> is 529.5 eV<sup>(32, 33)</sup>. The Y 3d spectrum exhibited a peak at 154.44 eV (figure 5c), whereas other tests have reported exhibition of a double peak at 158.8 and 156.8 eV resulting from spin-orbit splitting of the Y 3d<sub>3/2</sub> and Y 3d<sub>5/2</sub> levels for Y<sub>2</sub>O<sub>3</sub><sup>(5,10,26-29,31)</sup>, respectively. The peak at 154.44 eV (figure 5c) in the Y 3d spectrum, is from the Si 2s level<sup>(28-30, 32, 33)</sup>.

### *Scanning electron microscopy*

Figure 6 shows irregular shaped glass particles, whereas regular spherical particles are shown in figure 7. Illustrations shown in these figures confirm that silicone oil method as a novel procedure for the production of closed spherical particles. One advantage of this method over other methods<sup>(1, 12-14)</sup> is that high temperatures are not required. Moreover, large quantities of sphere are produced at a high rate, and isodiametric spheres can be synthesized that do not require screening.

As shown in figure 8, most of the particles obtained by the proposed method were approximately 20-50 μm in diameter. Therefore, the procedure used to produce this material can be determined as appropriate.

### *SEM/EDS mapping analysis*

Topographical analysis of cross-sections showed that these microspheres had a boiled egg structure. Figures 9 and 10 show the interior of microspheres and demonstrate they were composed of two primary layers, a crust and a core layer.

Figures 9 and 10 also show that Y and Al were

distributed primarily in the core, whereas Si was distributed in the crust, which appeared as a halo surrounding a microsphere. Oxygen distribution was approximately homogenous among all microspheres.

### SEM/EDS line scan analysis

Figures 11 and 12 show the SEM-EDX line scan analysis along a cross-section of the Azar samples for various concentrations of Si, Y, O and Al. Line scan analysis indicated that Si concentrations were higher at the beginning and end of the line, forming a U shape, while Si concentrations were lower in the middle of the line as a result of the presence of Y and Al.

Figures 11 and 12 show that the elements Y and Al were situated in the middle of the microspheres, providing further evidence of the boiled egg like structure of the microspheres produced by this method.

### Chemical analyzing

Table 1 shows the elements and table 2 shows composition of the Azar microspheres. These tables show that samples had low-level evaluations for impurities. Carbon impurity was about 0.02 % for Azar 1 and 0.01 % for Azar 2. La & Lu impurities were related to Y compound impurities.

## DISCUSSION

The method introduced above did not use high temperatures, so it presents a suitable procedure for the production of metallic microspheres that contain oxides with a high melting point, such as rhenium, holmium, samarium and lutetium microspheres. Moreover, the procedure presents an approach suitable for the production of non-metallic glass microspheres that contain oxides with a low boiling point, such as phosphate glass microspheres.

Due to the crust of silicon that forms around the microspheres, the proposed method is expected to be suitable for the production of radioactive seed sources for implantation in tumors and cancer tissue.

## CONCLUSION

Results indicate that the proposed method of silicone oil spheroidization is suitable for the production of yttrium glass microspheres.

## REFERENCES

1. Day DE, Gary R, Ehrhardt J (1988) Radioactive glass microspheres. U S Pat No 5011677.
2. Erbe EM and Day ED (1993) Chemical durability of  $Y_2O_3-Al_2O_3-SiO_2$  glasses for the *in-vivo* delivery of beta radiation. *J Biomed Mater Res*, **27**: 1301-1308.
3. Kawashita M, Miyaji F, Kokubo T, Takaoka GH, Yamada I, Suzuki Y, Kajiyama K (1997) Preparation of glass for radiotherapy of cancer by P + Ion implantation at 100 keV. *Nucl Instrum Meth Phys Res, B* **121**: 323-327.
4. Kawashita M, Miyaji F, Kokubo T (1999) Preparation of Phosphorus-Containing Silica Glass Microspheres for Radiotherapy of Cancer by Ion Implantation. *J Mater Sci Mater Med*, **10**: 459-463.
5. Kawashita M, Miyaji F, Kokubo T, Takaoka GH, Yamada I, Suzuki Y, Inoue M (1999) Surface structure and chemical durability of  $P^+$  - implanted  $Y_2O_3-Al_2O_3-SiO_2$  glass for radiotherapy of cancer. *J Non-Cryst Solids*, **255**: 140-148.
6. Kawashita M, Takayama Y, Kokubo T, Takaoka GH, Araki N, Hiraoka M (2006) Enzymatic preparation of hollow yttrium oxide microspheres for in situ radiotherapy of deep-seated cancer. *J Am Ceram Soc*, **89**: 1347-1351.
7. Kawashita M, Miyaji F, Kokubo T, Takaoka GH, Yamada I, Suzuki Y, Kajiyama K (1997) Preparation of radiotherapy glass by phosphorus ion implantation at 100 keV. *J Biomed Mater Res*, **38**: 342-347.
8. Kawashita M, Matsui N, Li Zh, Miyaza T (2010) Preparation of porous yttrium Oxide microparticles by gelation of ammonium alginate in aqueous solution containing yttrium ions. *J Mater Sci: Mater Med*, **21**: 1837-1843.
9. Christie JK and Tilocca A (2010) Short-range structure of yttrium alumino-silicate glass for cancer radiotherapy: Car-Parrinello Molecular Dynamics Simulations. *Adv Eng Mater*, **12**: B326-B330.
10. Simon V, Eniu D, Takácsb A, Magyar K, Neumannb M, Simon S (2005) X-Ray Photoemission Study of Yttrium Contained in Radiotherapy Systems. *J Optoelectron Adv Mater*, **7**: 2853-2857.
11. Heness G and Ben-Nissan B (2004) Innovative Bioceramics. *Mater Forum*, **27**: 104-114.
12. Sene FF, Martinelli JR, Okuno E (2008) Synthesis and characterization of phosphate glass microspheres for radiotherapy applications. *J Non-Cryst Solids*, **354**: 4887-4893.
13. Kawashita M, Shineha R, Kim HM, Kokubo T, Inoue Y, Araki N, Nagata Y, Hiraoka M, Sawada Y (2003) Preparation of ceramic microspheres for in situ radiotherapy of



- deep-seated cancer. *Biomate*, **24**: 2955-2963.
14. Sreekumar KP, Saxena SK, Kumar Y, Thiyagarajan TK, Dash A, Ananthapadmanabhan PV, Venkatesh M (2010) studies on the preparation and plasma spherodization of yttrium aluminosilicate glass microspheres for their potential application in liver brachytherapy. *J Phys Conf Ser*, **208**: 1-5.
  15. Mantravadi RVP, Spignos DG, Tan WS, Felix EL (1982) Intraarterial yttrium 90 in the treatment of hepatic malignancy. *Radiol*, **142**: 783-786.
  16. Cho SM, Kim YT, Yoon DH (2003) Optical characterization of silica based waveguide prepared by plasma enhanced chemical vapor deposition. *J Korean Phys Soc*, **42**: S947-S951.
  17. Karl A, Gschneidner Jr, Eyring LR (1986) Handbook on the physics and chemistry of rare earths. Vol 8 Elsevier Science Publishers B.V.
  18. Palanivel R and Velraj G (2007) FTIR and FT-Raman spectroscopic studies of fired clay artifacts recently excavated in Tamilnadu, India. *Indian J Pure & Appl Phys*, **42**: 501-508.
  19. Gradeff PS, Yunlu K, Deming TJ, Olofson JM, Doedens RJ, Evans WJ (1990) Synthesis of yttrium and lanthanide silyloxy complexes from anhydrous nitrate and oxo alkoxide precursors and the X-ray crystal structure of [Ce(OSiPh<sub>3</sub>)(THF)<sub>3</sub>](THF). *Inorg Chem*, **29**: 420-424.
  20. Chambers JJ (2000) Reactions for yttrium silicate high-K dielectrics. PHD theses, North Carolina State University, Raleigh.
  21. <http://vasculardiseasemanagement.com/content/does-microparticle-size-affect-bland-embolization-outcomes-local-treatment-liver-malignancy>
  22. Yang CS, Kim JS, Choi JW, Kwon MH, Kim YJ, Choi JG, Geug T Kim (2002) XPS study of aluminum oxides deposited on PET thin film. *J Ind and Eng Chem*, **6**: 149-156.
  23. Shpotyuk O, Filipecki J, Klym H, Ingram A (2009) Combined XRD, XPS and pALS characterization of humidity sensitive MgAl<sub>2</sub>O<sub>4</sub> ceramics. *Ser Phys*, **43**: 199-208.
  24. Van Den Brand J, Snijders PC, Sloof WG, Terryn H, de Wit JHW (2004) Acid-Base Characterization of Aluminum Oxide Surfaces with XPS. *J Phys Chem B*, **108**: 6017-6024.
  25. D. Niu, Ashcraft RW, and Parsons GN (2002) Water absorption and interface reactivity of yttrium oxide gate dielectrics on silicon. *Appl Phys Lett*, **80**: 3575-3577.
  26. Niu D, Ashcraft RW, Chen Z, Stemmer S, Parsons GN (2003) Chemical, physical, and electrical characterizations of oxygen plasma assisted chemical vapor deposited yttrium oxide on silicon. *J Electrochem Soc*, **150**: F102-F109.
  27. Zaharieva K and Vissokov G (2008) Preparation and characterization of plasma-chemically synthesized nanodispersed powders of ZrO<sub>2</sub>-Y<sub>2</sub>O<sub>3</sub> and SiO<sub>2</sub>. *Annu Univ Min Geol*, **51**: 87-91.
  28. Simon V, Eniua D, Takácsb A, Magyar K, Neumannb M, Simon S (2005) Iron doping on the electronic structure in yttrium aluminosilicate glasses. *J Non-Cryst Solids*, **351**: 2365-2372.
  29. Lide DR ed. (2007) CRC Handbook of Chemistry and Physics, 87<sup>th</sup> Edition. Taylor and Francis, Boca Raton, FL..
  30. Niu D (2002) Interface reactions during processing of chemical vapor deposited yttrium oxide high-k dielectrics. PHD Theses. North Carolina State University, Raleigh.
  31. Zhang H, Guo X, Zhang Q, Ma Y, Zhou H, Li J, Wang L, Deng Y (2008) Synthesis of dialkyl hexamethylenedicarbamate from 1,6-hexamethylenediamine and alkyl carbamate over Y(NO<sub>3</sub>)<sub>3</sub>·6H<sub>2</sub>O catalyst. *J Mol Catal A: Chem*, **296**: 36-41.
  32. Chambers JJ, Busch BW, Schulte WH, Gustafsson T, Garfunkel E, Wang S, Maher DM, Klein TM, Parsons GN (2002) Effect of surface pretreatments on interface structure during formation of ultra-thin yttrium silicate dielectric films on silicon. *Appl Surf Sci*, **181**: 78-93.
  33. Chambers JJ and Parsons GN (2001) Physical and electrical characterization of ultrathin yttrium silicate insulators on silicon. *J Appl Phys*, **90**: 918-933.
  34. Gulec SA and Siegel JA (2007) Post therapy radiation safety considerations in radiomicrosphere treatment with 90Y-microspheres. *J Nucl Med*, **48**: 2080-2086.

